

EVAPORATION OF METALLIC TARGETS CAUSED BY INTENSE OPTICAL RADIATION

V. A. BATANOV, F. V. BUNKIN, A. M. PROKHOROV and V. B. FEDOROV

P. N. Lebedev Physics Institute

Submitted February 25, 1972

Zh. Eksp. Teor. Fiz. 63, 586–608 (August, 1972)

A theory of evaporation of metals induced by an intense optical radiation beam is developed on the basis of the liquid-vapor phase transition. A method for approximate solution of the Clapeyron-Clausius equation is suggested which permits one to determine the temperature of the target surface as a function of incident radiation intensity I with sufficient, for experimental purposes, accuracy. It is shown that when a certain critical value of the intensity $I_{md} \sim (10^7 - 10^8 \text{ W/cm}^2)$ is exceeded a new effect, a "transparency wave," arises as a result of loss of metallic properties by the target: in the front of the wave the liquid metal changes into liquid dielectric. For $I > I_{md}$ vaporization begins to take place at the surface of the "transparent" (dielectric) layer, the temperature T_{md} of which ceases to increase and remains below the critical value. This layer is separated from the metal by the front of the transparency wave propagating into the target. This transparency effect is accompanied by the appearance of a number of other effects which may serve for its observation, viz., a sharp drop of the target reflection coefficient, a considerable change of the evaporation front velocity dependence on I , and finally the appearance of maximum followed by a monotonic decrease in the dependence of the specific recoil momentum on I . The latter effect was experimentally observed in the present investigation. The results are presented in the paper.

INTRODUCTION

It has been established by now with the aid of laser sources that the phase transition of a condensed substance into vapor is one of the possible mechanisms of disintegration of metals by powerful optical radiation^[1-4]. The absorption of light energy by the metal leads in this case to heating of the target surface layer to temperature of several thousand degrees. This results in intensive evaporation. The evaporation front (the phase separation boundary) moves into the interior of the target, and this is the cause of the disintegration of the target material in the irradiated zone.

The circle of physical processes that arise when powerful optical radiation interacts with metals is quite large. In addition to the phase transition on the evaporation front, it includes also phenomena in the plasma flare that is produced near the target surface as the result of heating of the metal vapor ejected from the target. It is of interest to investigate the gasdynamic picture of vapor motion in the flare and the characteristics of the flare plasma, which determine the coefficient of absorption of the light passing through it and the degree to which the target is screened against the incident radiation. We confine ourselves in the present article only to the evaporation kinetics, the phase transition, and the processes occurring in the interior of the target.

The paper consists of a theoretical part and an experimental part. The first part contains an exposition of the theory of the development of metal evaporation by a laser beam, on the basis of the liquid-vapor phase transition, in place of the solid-vapor model which is now widely used in the literature (see, e.g.,^[3]). We show that if the intensity of the incident radiation exceeds a certain threshold (for the fully-developed evaporation regime), then the temperature of the target surface and of a layer adjacent to it, with a typical

dimension $\chi/u \sim 10^{-3} \text{ cm}$ (χ is the temperature conductivity and u is the speed of motion of the evaporation front into the interior of the metal) is always higher than the normal boiling temperature of the metal, i.e., it is certainly higher than its melting temperature. Thus, the evaporation is from the liquid metal, and the solid-vapor model is not applicable¹⁾. At the same time, the difference between the two models is fundamental. Only within the framework of the liquid-vapor transition is it possible to consider the intensity region corresponding to a metal-surface temperature close to the critical temperature T_c .

It is shown in the present paper that when the radiation intensity is increased above a certain threshold value I_{md} , the temperature of the evaporating target reaches a value $T_{md} < T_c$ and ceases to increase further. At this temperature, the metallic conductivity ceases and the liquid metal becomes a liquid dielectric. As the result of the transition, the material of the target is "bleached" and becomes almost transparent to the incident radiation. The evaporation now proceeds already from the surface of a liquid dielectric at a fixed speed $u(T_{md})$ of the evaporation front, while the excess intensity over the loss to evaporation is consumed in detachment of the "induced transparency" front from the evaporation front and its motion into the interior of the target ("induced transparency" wave), with a speed $D > u(T_{md})$. The possibility of observing the evaporation regime with a transparency wave is discussed later on (see the end of Sec. 2).

We note that the foregoing results render incorrect the widely held concept (see^[3,4]) that an increase of I makes possible a monotonic heating of the target surface

¹⁾This is confirmed also by experiment, since sputtering of liquid metal is observed in all cases in addition to the evaporation of the target.

by absorption of radiation, up to temperatures $T \sim \lambda_1$ and above, where λ_1 is the evaporation energy per particle and its order of magnitude is $10T_c$ (^[5], Sec. 85). Temperatures $T > T_c$ can be reached only in vapor as a result of strong absorption of the incident radiation by the vapor.

The article contains experimental facts that demonstrate that the target surface reaches temperature close to critical, at which the mechanism of metallic absorption ceases and the metal turns into a dielectric. One of these results was obtained in the present study (see Sec. 4) and pertains to the anomalous dependence of the specific momentum of the vapor's recoil from the target on the light intensity for certain metals. Another fact was described but incorrectly explained from our point of view in ^[6], where an increase of the beam intensity was accompanied by a severalfold decrease of the coefficient of light reflection from the target in comparison with the value typical of metals.

"Saturation" of the growth of the evaporation front velocity in aluminum with increasing target radiation intensity above 2×10^7 W/cm² has been observed in experiments ^[7].

1. LIQUID-VAPOR PHASE TRANSITION

In this section we consider the evaporation of metals at light fluxes corresponding to target surface temperatures T lower than the critical temperature T_c .²⁾ Our analysis is based to a considerable degree on certain already known results concerning the kinetics of evaporation and establishment of hydrodynamic motion of vapor from an evaporating target ^[3,4,8]. Our main purpose is to examine in succession the development of evaporation, using the liquid-vapor model. This examination is needed in order to analyze the phenomena investigated in the succeeding sections. The material of the present section, from our point of view, is also of independent interest, since it deals with one of the most difficult aspects of our problem, the kinetics of evaporation, on a more realistic basis than in the past.

The regime of developed evaporation sets in at high values of the intensity I of the incident radiation, when the thermal-conductivity mechanism is excluded. The latter means that the energy is released in the surface layer of the material so rapidly that the material evaporates before the thermal-conductivity process is capable of carrying away the released heat from the layer. In such a regime, the speed u of the evaporation front is determined by an obvious formula that follows from energy considerations:

$$u = \frac{(1-R)I}{\lambda_{\text{eff}}} V, \quad (1)$$

where R is the coefficient of reflection of the radiation from the target surface, $V = 1/\rho$ is the specific volume of the liquid phase of the substance, ρ is its density, and λ_{eff} is a certain effective specific heat of evaporation and its value far from T_c is close to the true heat of evaporation λ at a steady-state target temperature T (the exact meaning of λ_{eff} will be determined below). Although in the regime under consideration the thermal-

conductivity mechanism is in fact excluded and does not affect, e.g., the speed u of the evaporation front, it does determine the thickness Δl of the layer heated to the surface temperature T , namely Δl of the layer heated to the surface temperature T , namely $\Delta l \sim \chi/u$. Under typical conditions $\Delta l \sim 10^{-3}$ cm. As will be shown below, the temperature of this layer always exceeds the normal boiling temperature, and consequently the evaporation always proceeds from the liquid phase.

The regime of developed evaporation has a threshold with respect to the intensity of the incident radiation. Its value I_{thr} is estimated from the following considerations. Let $\Delta \mathcal{E}$ be the increment of the internal specific energy of the substance on the target boundary, resulting from its irradiation during a time t in the thermal conductivity regime (i.e., at sufficiently low irradiation intensities I). For the case of greatest practical interest, when $\sqrt{\chi t} \ll L$, h and $a \ll L$, where a is the radius of the irradiated spot, and L and h are respectively the transverse dimension of the target and its thickness (the target is an "infinite half-space"), the increment $\Delta \mathcal{E}$ for different irradiation-time intervals at constant intensity I is given by (see ^[9], p. 259)

$$\Delta \mathcal{E} = \begin{cases} (1-R)I\rho^{-1}\delta^{-1}t, & t \ll \delta^2/\chi; \\ (1-R)I\rho^{-1}\sqrt{t/\chi}, & a^2/\chi \gg t \gg \delta^2/\chi; \\ (1-R)I\rho^{-1}\chi^{-1}a, & t \gg a^2/\chi. \end{cases} \quad (2a)$$

$$\Delta \mathcal{E} = \begin{cases} (1-R)I\rho^{-1}\delta^{-1}t, & t \ll \delta^2/\chi; \\ (1-R)I\rho^{-1}\sqrt{t/\chi}, & a^2/\chi \gg t \gg \delta^2/\chi; \\ (1-R)I\rho^{-1}\chi^{-1}a, & t \gg a^2/\chi. \end{cases} \quad (2b)$$

$$\Delta \mathcal{E} = \begin{cases} (1-R)I\rho^{-1}\delta^{-1}t, & t \ll \delta^2/\chi; \\ (1-R)I\rho^{-1}\sqrt{t/\chi}, & a^2/\chi \gg t \gg \delta^2/\chi; \\ (1-R)I\rho^{-1}\chi^{-1}a, & t \gg a^2/\chi. \end{cases} \quad (2c)$$

Here δ^{-1} is the coefficient of radiation absorption in the target material ($\delta \sim 10^{-4}-10^{-5}$ cm for metals). The threshold intensity I_{thr} is determined from this formula by putting in it formally $I = I_{\text{thr}}$ and $\Delta \mathcal{E} = \lambda_{\text{eff}}$. We then obtain

$$I_{\text{thr}} \approx \begin{cases} \lambda_{\text{eff}}\rho(1-R)^{-1}\delta/t, & t \ll \delta^2/\chi; \\ \lambda_{\text{eff}}\rho(1-R)^{-1}\sqrt{\chi/t}, & a^2/\chi \gg t \gg \delta^2/\chi; \\ \lambda_{\text{eff}}\rho(1-R)^{-1}\chi/a, & t \gg a^2/\chi. \end{cases} \quad (3a)$$

$$I_{\text{thr}} \approx \begin{cases} \lambda_{\text{eff}}\rho(1-R)^{-1}\delta/t, & t \ll \delta^2/\chi; \\ \lambda_{\text{eff}}\rho(1-R)^{-1}\sqrt{\chi/t}, & a^2/\chi \gg t \gg \delta^2/\chi; \\ \lambda_{\text{eff}}\rho(1-R)^{-1}\chi/a, & t \gg a^2/\chi. \end{cases} \quad (3b)$$

$$I_{\text{thr}} \approx \begin{cases} \lambda_{\text{eff}}\rho(1-R)^{-1}\delta/t, & t \ll \delta^2/\chi; \\ \lambda_{\text{eff}}\rho(1-R)^{-1}\sqrt{\chi/t}, & a^2/\chi \gg t \gg \delta^2/\chi; \\ \lambda_{\text{eff}}\rho(1-R)^{-1}\chi/a, & t \gg a^2/\chi. \end{cases} \quad (3c)$$

The value of I_{thr} determined in this manner depends on the time t . The meaning of this dependence is as follows. If a radiation pulse of duration τ has an intensity $I < I_{\text{thr}}(\tau)$, then no developed-evaporation regime sets in when it is incident on the target. On the other hand, if $I > I_{\text{thr}}(\tau)$, then developed evaporation sets in during a time $t^* \lesssim \tau$, determined from the condition $I_{\text{thr}}(t^*) = I$, and lasts until the end of the pulse. Figure 1 shows a characteristic plot of I_{thr} against the irradiation time t .

In experiments on evaporation of metals by pulsed laser radiation, the intermediate case is usually realized, with $a^2/\chi \gg t \gg \delta^2/\chi$, and the corresponding formula (3b) for I_{thr} is well known (see ^[4]). It yields

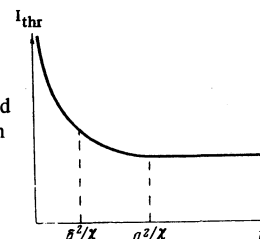


FIG. 1. Typical plot of the threshold intensity I_{thr} for developed evaporation vs the irradiation time t (one-dimensional evaporation).

²⁾The limits of applicability of the theory developed in the present section are indicated more rigorously in Sec. 2.

for the threshold intensity an estimate that agrees with the experimental data, namely $I_{\text{thr}} \sim 10^6 \text{ W/cm}^2$ for most metals at laser pulse durations $\tau \sim 10^{-3} \text{ sec}^3$.

In the quasicontinuous regime, when the third case is realized ($t \gg a^2/\chi$), the threshold intensity can be appreciably decreased; for metals at a $\sim 1 \text{ cm}$ it amounts to $I_{\text{thr}} \sim 10^5 \text{ W/cm}^2$ (with $t \gg 1 \text{ sec}$). We note also that the first case, in which $t \ll \delta^2/\chi$, occurs usually in pulsed evaporation of nonmetals. Then, as seen from (3), the evaporation has a threshold not with respect to the intensity of the incident pulse but with respect to its energy density $E = It$.

The temperature T of the evaporating surface is determined by the balance between the absorbed power $(1 - R)I$ and the rate of energy loss due to evaporation. To find the $T(I)$ dependence, it is necessary to supplement (1) with an equation connecting the conserved flux of matter $j_1 \equiv u/V$ with the temperature T (in this case λ_{eff} is regarded as a known function of T). Were there no backward flow of evaporated particles to the target, then this connection would be determined by the known expression for the evaporation flux in a vacuum (see, e.g.,^[5], Sec. 81):

$$j_{\text{vac}} = P_s(T) \sqrt{M/2\pi T}, \quad (4)$$

where M is the mass of the atom and $P_s(T)$ is the saturated-vapor pressure at the temperature T . In fact, as shown in^[6] (see also^[3], Sec. 4.1), there is always a backward flow, but it is small and for metals (particle adhesion coefficient $\beta \approx 1$) it amounts to approximately 18%. This means that $j_1 = 0.82j_{\text{vac}}$, and we obtain on the basis of (1) and (4) the following equation for $T(I)$:

$$I(1 - R) = 0.82\lambda_{\text{eff}}(T)P_s(T) \sqrt{M/2\pi T}. \quad (5)$$

The functions $\lambda_{\text{eff}}(T)$ and $T_s(T)$ are then assumed to be known; $T_s(T)$ can be determined by solving the Clapeyron-Clausius equation (see below), and $\lambda_{\text{eff}}(T)$ on the basis of a rigorous derivation of formula (1), based on the conservation laws for the flow of energy, momentum, and matter through the discontinuity between the liquid phase of the substance and the region of steady hydrodynamic motion of the vapor. These laws yield respectively

$$I(1 - R)/j_1 = w_1(T_1) - w(T) + \frac{1}{2}j_1^2(V_1^2 - V^2) + \int_{T_1}^T C dT, \quad (6a)$$

$$P = P_1 + j_1^2(V_1 - V), \quad (6b)$$

$$j_1 \equiv u/V = u_1/V_1. \quad (6c)$$

Quantities without subscripts pertain here to the condensed phase (ahead of the discontinuity) and those marked with the subscript 1 pertain to the region of steady flow of the vapor (behind the discontinuity); w is the specific enthalpy, V is the specific volume, P is the pressure, u is the speed of the evaporation front, and u_1 is the speed of the steady-state (one-dimensional) vapor motion and equals the local speed of sound, i.e., $u_1 = (\gamma T_1/M)^{1/2}$ ($\gamma = 5/3$ is the adiabatic exponent). The integral in the right-hand side of (6a) takes into account the energy needed to heat the metal from the initial

(room) temperature T_2 to the temperature of developed evaporation T (we neglect the loss due to the latent heat of melting), and C is the specific heat of the condensed phase.

Comparison of (6a) and (1), with (6c) taken into account, shows that

$$\begin{aligned} \lambda_{\text{eff}}(T) &= w_1(T_1) - w(T) + \frac{1}{2}j_1^2(V_1^2 - V^2) + \int_{T_1}^T C dT \\ &= \lambda(T) - \frac{5}{2M}(T - T_1) + \frac{5}{6M}T_1 + \int_{T_1}^T C dT. \end{aligned} \quad (7)$$

When writing down the second equation, we used, first, the definition of the specific heat of evaporation $\lambda(T) \equiv w_1(T) - w(T)$, and second $w_1(T) = C_p T = (5/2M)T$ and $V_1 \gg V$.

The connection between the temperature T_1 and the specific volume V_1 of the vapor, on the one hand, and the target temperature T on the other, is obtained by solving the corresponding kinetic problem. This was done in^[8] (^[3], Sec. 4.1), where it was shown that

$$T_1 = 0.65T, \quad 1/V_1 = 0.31/V, = 0.31MP_s(T)/T; \quad (8)$$

here V_s is the specific volume of the saturated vapor. Substitution of T_1 from (8) in (7) leads to a final expression for $\lambda_{\text{eff}}(T)$:

$$\lambda_{\text{eff}}(T) = \lambda(T) + \int_{T_1}^T C dT - 0.35T/M. \quad (9)$$

Far from the critical point the increment to $\lambda(T)$ in the right-hand side of (9) is negligibly small, since the second term is $\approx 3T/M$ and $\lambda(T)$ in this region is constant and is approximately equal to $10T_c/M$ (the third term can always be neglected). Near the critical point, where $\lambda(T)$ begins to decrease (like $\sqrt{T_c - T}$), identification of λ_{eff} with λ can lead, generally speaking, to an appreciable error. However, when $T(I)$ is determined from Eq. (5), such an identification is always possible without incurring a large error, even in the vicinity of the critical point, if the heat of evaporation λ is assumed to be independent of the temperature and its value is assumed to be the same as far from T_c , e.g. at the normal boiling temperature T_0 . In fact, far from T_c we should obtain a result that is certainly correct (since $\lambda_{\text{eff}}(T) \approx \lambda(T_0)$), and near T_c , where $\lambda_{\text{eff}}(T)$ may turn out to be several times smaller than $\lambda(T_0)$, such a substitution leads only to a logarithmic error, as is seen from Eq. (5) when allowance is made for the fact that $P_s \sim \exp(-\lambda_0/T)$ (see (12)). For the same reason, the numerical coefficient 0.82 of (5) is not of great importance in the $T(I)$ dependence and will henceforth be omitted.

Before we proceed to find $P_s(T)$, we call attention to the fact that since the backward flux of the particles to the target is small, it follows that the pressure exerted on the target in the developed evaporation regime is close to $P_s(T)/2$. Since the pressure does not experience a discontinuity on the evaporation surface itself, its value inside the target is also close to $P_s(T)/2$. A rigorous calculation by means of formula (6b) with allowance for (8), leads to (^[3], Sec. 4.1):

$$P = P_1(1 + \gamma) = T_1(1 + \gamma)/MV_1 = 0.56P_s(T). \quad (10)$$

Thus, in the fully developed evaporation the observed liquid-vapor phase transition is always far from equili-

³At $I > I_{\text{thr}}(\tau)$, the time of development of the developed evaporation is $t^* \approx \tau [I_{\text{thr}}(\tau)/I]^2$. $t^* \ll \tau$ if the threshold is exceeded by several times.

brum. The liquid phase is in a superheated state. For the questions considered in the present section, however, this circumstance is apparently of no importance, for no boiling can develop inside the volume during the lifetime $\sim \chi/u^2$ of the liquid-metal layer, owing to the large values of the surface-tension coefficients of liquid metals.

To find $P_S(T)$, we use the Clapeyron-Clausius equation in the form

$$P_S^{-1} dP_S / dT = \lambda_1(T) / \Delta Z(T) T^2, \quad (11)$$

where $\lambda_1(T) = M\lambda(T)$ is the heat of evaporation per particle, and $\Delta Z = (P_S/T)(v_{\text{vap}} - v_{\text{liq}})$ is the difference between the compressibility coefficients of the vapor and the liquid (v_{vap} and v_{liq} are respectively the volumes of the gas and liquid phases per particle). The advisability of writing down the Clapeyron-Clausius equation in form (11) and of introducing the quantity $\Delta Z(T)$ follows from the experimental fact that for most liquids (including liquid metals) the ratio $\lambda_1(T)/\Delta Z(T)$ remains approximately constant in the temperature interval $T_0 \leq T \leq T_C$ (with different accuracy for different liquids)⁴⁾. Far from T_C , where $\Delta Z \approx 1$ ($v_{\text{vap}} \gg v_{\text{liq}}$)⁵⁾, this fact is due to the weak temperature dependence of the heat of evaporation λ_1 ; in the vicinity of T_C it is due to the fact that the quantities $\lambda_1(T)$ and $\Delta Z(T)$ tend to zero in equal fashion as $T \rightarrow T_C$ (like $\sqrt{T_C - T}$; see^[5], Sec. 84).

Although the temperature interval in which the ratio $\lambda_1/\Delta Z$ remains constant is relatively small (we recall that $T_0 \approx (0.6-0.7)T_C$), this circumstance is quite important for the problem of fully developed evaporation, since (as will be shown below) in this evaporation regime the target temperature T is always located just in the interval $T_0 < T < T_C$, so that we can use in (5) a $P_S(T)$ dependence that is valid only in the indicated interval. This dependence, in turn, can be obtained by solving Eq. (11) under the assumption that $\lambda_1/\Delta Z = \text{const}$.

Putting $\lambda_1/\Delta Z = \lambda_1(T_0) \equiv \lambda_0 = \text{const}$, we obtain on the basis of (11) the following relation that is valid in the interval $T_0 \leq T \leq T_C$:

$$P_S(T) = (P_0 e^{\lambda_0/T_0}) e^{-\lambda_0/T} \equiv \varphi_0 e^{-\lambda_0/T}, \quad (12)$$

where $P_0 = 1$ atm. The condition $\lambda_0/\Delta Z = \text{const}$ reflects definite thermophysical properties of the liquid (and also of dense vapor) in the considered temperature interval, sufficient to construct a theory of developed evaporation on the basis of the liquid-vapor transition. It is seen from (12) that to determine $P_S(T)$ in this interval it is necessary to know only two thermophysical constants of the liquid, T_0 and λ_0 , which for most metals have been measured and are listed in handbooks. An indirect verification of the validity of (12) up to the critical temperature is afforded by the fact that the

⁴⁾For water and many organic liquids, these data are given in [10], and for metals (mercury and cesium) the constancy of $\lambda_1/\Delta Z$ follows from the fact that the measured values of $T_S(T)$, up to T_C (see [11]) agree well with the solution of Eq. (11) at $\lambda_1/\Delta Z = \text{const}$.

⁵⁾We note that the condition $v_{\text{vap}} \gg v_{\text{liq}}$ is sufficient for the vapor to be regarded as an ideal gas (see [12], p. 195). This condition is usually satisfied up to temperatures T sufficiently close to T_C , since the principal change in the density of the liquid phase occurs in the immediate vicinity of the critical state (see Fig. 3 of Sec. 2).

known data on P_C and T_C of different metals (see^[13]) agree sufficiently well with this formula.

It should be noted that the general form of expression (12) for the saturated vapor pressure, $P_S \sim \exp(-\lambda_0/T)$, is well known, but in numerical calculations one encounters the problem of correctly choosing the exponent λ_0 and the pre-exponential term. We have shown above how to do this for fully developed evaporation of metals under the influence of optical radiation. The solid-vapor transition model, which was used earlier in other studies (see^[3]) does not provide the correct answer to this question in our problem (i.e., in the temperature interval $T_0 < T < T_C$). The pre-exponential term obtained by that approach (see^[3], Sec. 4.1) depends on the temperature and is larger than φ_0 in (12) by approximately two or three orders of magnitude for all metals in the temperature interval under consideration. In addition, λ_0 in^[3] has the meaning of the heat of evaporation at $T = 0$. Such a discrepancy leads to considerable errors in the determination of the target temperature $T(I)$ and other parameters of the problem (vapor pressure, vapor density, etc.) when the solid-vapor model is used.

Substituting the obtained $P_S(T)$ dependence in (5), we obtain the final form of the relation between the target temperature T and the incident-radiation intensity I :

$$\exp(\lambda_0/T) = (I_\phi/I) (\lambda_0/T)^{1/2}, \quad (13)$$

where

$$I = \frac{P_0 \lambda_0^{1/2} \exp(\lambda_0/T_0)}{(1-R)\sqrt{2\pi M}}$$

(as explained above, the term $0.82\lambda_{\text{eff}}$ has been replaced by $\lambda(T_0)$). It is easy to show that for metals the solution $T(I)$ of this equation satisfies the condition $T(I) > T_0$ at $I > I_{\text{thr}}$. Indeed, substituting in (13) in place of I the expression (3b) for I_{thr} , we obtain the inequality

$$\lambda_0(T_0^{-1} - T^{-1}) > \ln \mathcal{R}, \quad \mathcal{R} \equiv (2\pi\chi T \rho^2 / M\tau P_0^2)^{1/2}.$$

It follows therefore that at

$$\mathcal{R}_0 = \mathcal{R}(T_0) > 1 \quad (14)$$

the target temperature is $T(I) > T_0$. The quantities ρ , χ , and T_0 in this inequality are well known for most metals so that the satisfaction of (14) can be verified directly. At radiation-pulse durations $\tau \sim 10^{-3}$ sec, such a verification for the metals used so far in experiments on evaporation shows that the inequality (14) is satisfied with a large margin (see the table⁶⁾). Thus, $T(I) > T_0 > T_m$ (T_m is the melting temperature).

Metal	ρ , g/cm ³	χ , cm ² /sec	T_0 , °K	\mathcal{R}	Metal	ρ , g/cm ³	χ , cm ² /sec	T_0 , °K	\mathcal{R}_0
Al	2.7	0.74	2894	20.2	Cu	8.96	1.15	3150	58
Bi	9.8	0.068	1750	6.3	Mo	10.2	0.53	5100	50
W	19.3	0.6	5650	73	Ni	8.9	0.225	2420	23
Fe	7.8	0.126	3050	17.7	Sn	7.3	0.364	3000	11.3
Mg	1.74	0.68	1380	9.3	Pb	11.3	0.236	2000	14.2
					Zn	7.13	0.278	1190	13.7

⁶⁾It is impossible to prove the inequality (14) in general case, but its satisfaction for metals becomes clearer if its left-hand side is represented in another (equivalent) form $[\eta_{\text{liq}}/\eta_{\text{L}}]^2 (2\pi\chi M/T_0\tau) (T_0/T^{(0)})^2 > 1$, where $\eta_{\text{L}} = 2.7 \times 10^{19}$ cm⁻³ is the Loschmidt number, η_{liq} is the density of the liquid, and $T^{(0)} = 300^\circ\text{K}$. For metals at $\tau \sim 10^{-3}$ sec, the factor in the square brackets is ≥ 1 .

Nowhere in this section did we take into account the absorption of light in the metal vapor. We shall show in our subsequent papers that in the case of evaporation in vacuum the incident radiation is screened by the vapor mainly in the region adjacent to an irradiated spot on the target, with dimensions on the order of $d = 2a$. It follows from general considerations that the optical thickness of this region depends little on the intensity I and its order of magnitude is $\theta \equiv \alpha d \approx 1$ (α is the coefficient of light absorption in the plasma). In fact, θ can not be much larger than unity in the stationary evaporation regime, since the condition $\theta \gg 1$ leads to a decrease in the flux of the evaporated particles, and consequently also to a decrease of α . To the contrary, when $\theta \ll 1$ the evaporation increases the absorption coefficient⁷⁾. For estimating purposes we put $\theta \approx 1$. The choice of this value of absorption agrees, in particular, with measurements of the specific recoil momentum (see Sec. 4).

In concluding this section we present plots of the target surface temperature against the initial radiation power flux $I_0 = Ie^{\theta}$, calculated for bismuth, lead, and aluminum in accordance with formula (13) at $\theta \approx 1$ (Fig. 2).

2. INDUCED TRANSPARENCY WAVE IN METAL

In this section we consider evaporation in the region of large radiation flux densities, when the target surface is heated to near-critical temperatures.

The main fact for the understanding of the physical phenomena of the target at high intensities and at temperatures $T \approx T_C$ is the vanishing of the metallic conductivity and of the high reflection and absorption coefficients associated with this conductivity. This fact was established earlier by Kikoin and Senchenkov^[15] independently of experiments on evaporation of metals by optical radiation (see also the review^[11]); they investigated experimentally the electric conductivity and the equation of state in a wide range of pressures and temperatures, including the critical state. They have shown that the conductivity is determined mainly by the density of the material. When the density drops below a certain value $\rho = \rho_{md} > \rho_c$, the conductivity σ vanishes jumpwise (it decreases by several orders of magnitude), and the liquid metal turns into a liquid dielectric. There is every reason for assuming that the behavior of the electric conductivity of mercury, observed in^[15], is common to all metals⁸⁾. The jumpwise vanishing of metallic conductivity is physically connected with the strong dependence of the electron collectivization on the density (on the average distance between the atoms); this dependence governs all the metallic properties of substances. The transition from a liquid metal into a liquid dielectric is in essence the inverse of Mott's transition; its feasibility, from the point of view of the theory of

⁸⁾ Similar results were obtained also for cesium (see [11]), but for this metal the vanishing of the metallic conductivity in the vicinity of the critical point is offset to a considerable degree by the appearance of plasma conductivity because of the low ionization energy of cesium.

⁷⁾ The condition $\theta \ll 1$ also contradicts our experimental data on the heating of the vapor near the target in a region with dimensions $\sim d$ by laser radiation (see the Conclusion). A preliminary report on this data is contained in [14].

FIG. 2. Target surface temperature T vs incident-light intensity I_0 for bismuth, lead, and aluminum in the region $I < I_{md}$ and $T < T_{md}$ (see Sec. 2).

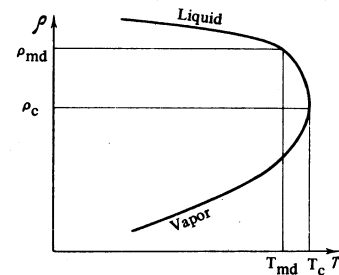
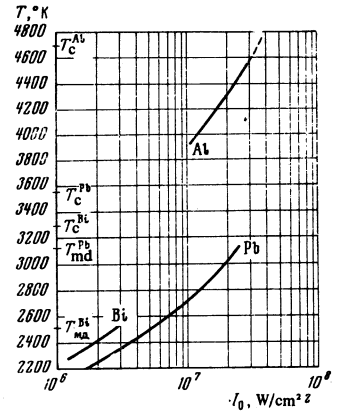


FIG. 3

phase transitions, was considered purely phenomenologically by Zel'dovich and Landau^[16] already back in 1944⁹⁾.

In experiments on the evaporation of metals by radiation, the relation between the liquid-metal density at the surface of the target in the region $\rho \gtrsim \rho_{md}$ and the target temperature T is quite close to that corresponding to phase equilibrium $\rho = \rho(T)$ (see Fig. 3), although, as noted in the preceding section (see (10)), the pressure in the metal is approximately half the equilibrium value. This is due to the low compressibility of the liquid, a property that remains in force down to the density value ρ_{md} (in accordance with the physical meaning of this quantity itself)¹⁰⁾. A sharp decrease of the density and the associated sharp increase of the compressibility occurs only in the immediate vicinity of T_C . For mercury, e.g., this vicinity is the approximate interval from $0.9 T_C$ to T_C ^[15].

The isochore $\rho = \rho_{md}$ crosses the curve $\rho = \rho(T)$ at the point $T = T_{md}$. The value of T_{md} when used in (13) determines the incident-radiation intensity threshold $I = I_{md}$, above which the liquid metal turns into a liquid dielectric. The target surface temperature does not rise in this case much above T_{md} ; and the excess of the radiation intensity above I_{md} goes to move the front of the induced transparency wave into the interior of the target. The general picture arising when $I > I_{md}$ is shown schematically in the upper half of Fig. 4.

The evaporation front now separates the liquid-dielectric region from the vapor and moves with constant velocity $u(T_{md})$. Detached from the evaporation front is an induced transparency wave that moves into

⁹⁾ For example, Mott's transition was experimentally revealed in [17] by a burst of metallic conductivity in paraffin and other insulators compressed in strong shock waves.

¹⁰⁾ The ratio is $\Delta\rho/\rho \sim 10^{-4} - 10^{-3}$ at $\Delta P = P_g/2 \sim 10^2 - 10^3$ atm.

the interior of the target and in the front of which the metal is initially heated and melted, and is then transformed into a dielectric.

It follows from the foregoing analysis that the mechanism of metallic absorption of light does not make it possible to heat the target above $T_{md} \lesssim T_c$. An increase in the incident-light intensity only increases the velocity of the induced-transparency wave.

It should be noted that the velocity of the induced-transparency wave is determined in final analysis by the rate of expansion of the matter in the front of the wave, and this rate cannot exceed the speed of sound. Consequently, the region of applicability of the foregoing exposition is bounded from above by intensity values at which the velocity of the induced-transparency wave does not exceed the velocity of sound in the cold metal. Other possible limitations will be considered at the end of the present section.

Before we proceed to a quantitative description of the induced-transparency wave, let us see how the conditions for the reflection and absorption of the light incident on the target change when its intensity goes through the point I_{md} . The complex dielectric constant of the target material at densities ρ both smaller and larger than ρ_{md} can be represented in the form

$$\epsilon' = \epsilon_0(1 - \omega\tau_0\xi + i\xi),$$

where $\xi = 2\sigma/\epsilon_0\nu$ (σ is the conductivity and $\nu = \omega/2\pi$ is the radiation frequency), τ_0 is the conduction-electron relaxation time, and ϵ_0 is the dielectric constant of the "lattice," i.e., of the ion core in the case when the material is in the metallic state ($\rho > \rho_{md}$) and of the dielectric liquid itself when the metallic conductivity vanishes ($\rho < \rho_{md}$, $\xi \ll 1$). It is assumed in all cases that the frequency ν lies far from the "lattice" absorption line and that accordingly ϵ_0 is real. On going from the state $\rho > \rho_{md}$ into the state $\rho < \rho_{md}$, the quantity ϵ_0 , as well as the conductivity σ , experiences a jump. However, if σ changes in this case by several orders of magnitude, so that $\xi(\rho > \rho_{md}) \gg 1$, and $\xi(\rho < \rho_{md}) \ll 1$, then the magnitude of the jump is $\Delta\epsilon_0 \ll \epsilon_0$, i.e., $\epsilon_0(\rho < \rho_{md}) \approx \epsilon_0(\rho > \rho_{md})$. This follows from the very definition of ϵ_0 . The relaxation time τ_0 , generally speaking, depends on the metal temperature, but it can be regarded as constant in the narrow interval $T_0 < T < T_{md}$ of interest to us. In the visible and in the near IR bands, for the considered temperature range of a liquid "good" metal, the parameter $\omega\tau_0$ is of the order of unity, as will henceforth be assumed¹¹.

The Fresnel coefficient R of reflection from the boundary of the material with dielectric constant ϵ' is determined by the well known formulas (see, e.g.,^[18], Secs. 63 and 66):

$$R = [(n-1)^2 + \kappa^2] / [(n+1)^2 + \kappa^2]. \quad (15)$$

where the refractive index n and the absorption coefficient κ are connected with ϵ' as follows:

$$\left. \begin{matrix} n \\ \kappa \end{matrix} \right\} = \sqrt{\epsilon_0/2} [(b^2 + \xi^2)^{1/4} \pm b]^{1/2}, \quad b = 1 - \omega\tau_0\xi. \quad (16)$$

¹¹We recall that for "good" conductors at room temperature the relaxation time is $\tau_0 \approx 3 \times 10^{-14}$ sec. Recognizing that τ_0 of pure metals is proportional to K/T , where K is the modulus of hydrostatic compression and decreases by several times on going over to the liquid state, we obtain a value $\tau_0 \sim 10^{-15}$ sec in the region of $T \approx 3000^\circ\text{K}$.

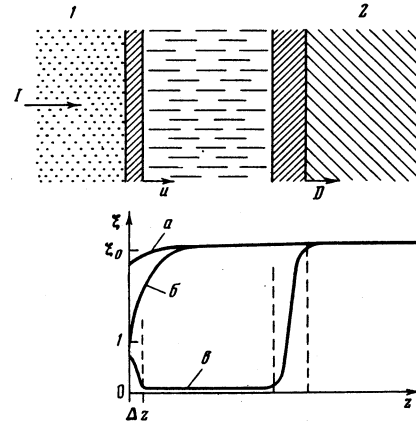


FIG. 4. Qualitative picture of evaporation in the induced-transparency regime $I > I_{md}$ (top) and variation of the parameter ξ in the interior of the target (bottom) at a fixed instant of time. u is the velocity of the interface between the vapor 1 and the liquid dielectric relative to the "cold" metal 2, D is the velocity of the induced-transparency wave in the same reference frame. a—variation of ξ at $I \ll I_{md}$ (the value $\xi_0 \gg 1$ corresponds to the state of a "good" metal), b—variation of ξ at $I = I_{md}$, c—variation of ξ at $I \gg I_{md}$ (the value of ξ increase to ξ_0 in the front of the induced-transparency wave).

In the evaporation regime at $I < I_{md}$, the target surface remains a metal, and consequently $\xi \gg 1$. The real part ϵ' is then negative and large in absolute magnitude (as is also its imaginary part). This circumstance, as is well known, results in a high coefficient R of reflection from the metal surface; the absorption coefficient μ , which determines the depth of penetration of the radiation into the medium ($1/\mu$) is also large in this case: $\mu_M = 2k_0\kappa \sim k_0\sqrt{\xi} > k_0$ ($k_0 = \omega/c$)¹². At the point $I = I_{md}$ ($\rho = \rho_{md}$, $T = T_{md}$) we have $\xi \approx 1$. The Fresnel reflection coefficient R then decreases abruptly and its value for all initially "good" metals is approximately 0.2. Indeed, we see from (16) that at $\xi \approx 1$ and $\omega\tau_0 \approx 1$ we have $n \approx \kappa \approx \sqrt{\epsilon_0/2} \approx 1$ (since $\epsilon_0 \approx 2$ far from the absorption line for all condensed media). Formula (15) then yields $R \approx 1/5$. At $\xi \approx 1$, however, the coefficient of absorption in the medium still remains large: $\mu \approx 2k_0$.

The medium becomes transparent at $I > I_{md}$, when the parameter ξ becomes small. The coefficient of light reflection from the evaporation boundary (dielectric-vapor) continues to decrease from its value $R = R_1$ at $\xi \approx 1$ and tends (at $I > I_{md}$) to the limiting Fresnel value $R_0 \equiv R(\xi = 0) = [(\sqrt{\epsilon_0} - 1)/(\sqrt{\epsilon_0} + 1)]^2 \approx 3 \cdot 10^{-2}$. The absorption coefficient in the transparent layer, according to (16) is $\mu_d = 2k_0\kappa \approx \epsilon_0^{1/2}k_0\xi \ll k_0$. Reflection from the induced-transparency wave, which propagates at $I > I_{md}$ into the interior of the target, is always small and can be disregarded since the transition from $\xi \ll 1$ to $\xi \gg 1$ is always sufficiently smooth (over a

¹²At $\xi \gg 1$, as follows from (16), we have $n \approx \kappa$, and formula (15) yields

$$R = 1 - \frac{4}{1 + (\kappa/n)^2} \frac{1}{n} + \frac{4}{[1 + (\kappa/n)^2]^2} \frac{1}{n^2}, \dots$$

where

$$\left. \begin{matrix} n \\ \kappa \end{matrix} \right\} = \sqrt{\epsilon_0/2} \sqrt{(1 + \omega^2\tau_0^2)^{1/4} \mp \omega\tau_0}.$$

For a very "good" metal, when $\sqrt{\xi} \gg 1$, we have $n \approx \kappa \gg 1$ and we can use the first term of the expansion (15*). The absorption coefficient is $\mu_M = (2/\delta_0) \sqrt{(1 + \omega^2\tau_0^2)^{1/2} + \omega\tau_0} \sim k_0 \sqrt{\xi}$; $\delta_0 = c/\sqrt{2\pi\omega\sigma}$.

distance spanning many wavelengths in the medium). Thus, the transition from the regime of simple evaporation ($I < I_{md}$) to the regime of evaporation with an induced-transparency wave ($I > I_{md}$) is characterized by a sharp decrease of the reflection coefficient R from the target (by not less than a factor of 5 for "good" metals). This can serve as the basis for an experimental observation of the effect under consideration (see Sec. 3).

The low value of the coefficient of reflection from the boundary of the evaporation front at $I > I_{md}$ does not mean that the entire radiation energy incident on the target reaches the induced-transparency front. Even if we neglect the volume absorption in the dielectric layer itself (the value of this absorption is determined not only by the absorption coefficient $\mu_d = \epsilon_0^{1/2} k_0 \xi$, but also by the thickness l_d of the dielectric layer, and under real observation conditions can be small enough: $\mu_d l_d \ll 1$), then the intensity of the radiation incident on the transparency front is $I_1 = (1 - R)I - (1 - R_1)I_{md}$, where $I = I_0 e^{-\theta}$ is the intensity of the radiation incident on the evaporation front, and R is the coefficient of reflection from this front at $I > I_{md}$, and its values depend on I and lie in the interval $R_1 > R > R_0$. This follows from the fact that to maintain the evaporation stationary at the surface temperature $T \approx T_{md}$ it is necessary that the same intensity $(1 - R_1)I_{md}$ (in accordance with the definition of I_{md}) be absorbed in the surface layer. The physical absorption mechanism is such that in a certain layer of thickness ΔZ , immediately adjacent to the evaporation boundary, there is established a lower temperature than in the interior of the transparent layer. The difference between these temperatures is smaller the larger the excess of I over $(1 - R_1)I_{md}$. The corresponding established distribution of the parameter ξ is shown in the lower half of Fig. 4. On the evaporation boundary itself we have $\xi = \xi(I) \lesssim 1$ even at $I > I_{md}$. The thickness ΔZ is determined by the kinetic processes of evaporation and should not depend on the intensity. The reflection coefficient R is determined by the conditions of reflection of the radiation from a flat layer with optical thickness $\psi = k_0 \Delta Z \sqrt{|\epsilon'(\xi)|}$, and the value $\xi = \xi(I)$ is established automatically in the layer in such a way that the same power is absorbed in the layer:

$$(1 - R_1)I_{md}, \text{ i.e., } 2k_0 \Delta Z \kappa(\xi)I = (1 - R_1)I_{md}$$

The optical thickness of the layer is $\psi \approx k_0 \Delta Z \kappa \ll 1$, and the coefficient R of reflection from this layer can be represented in the form (see^[18], Sec. 66)

$$R \approx 4R_1 \psi^2 \approx R_1 (1 - R_1)^2 (I_{md}/I)^2.$$

(It is assumed that $\xi \ll 1$ and $R_0 = 0$ in the interior of the dielectric.) Since $R_1 \ll 1$, this formula can be regarded as approximately correct in the entire interval $I > I_{md}$. We see from it that at $I > I_{md}$ the coefficient of reflection from the target decreases like $1/I^2$. Such a law governing the decrease of R must be regarded as slow in comparison with the preceding jumplike change of R from R_m to R_1 (from $\xi \gg 1$ to $\xi \ll 1$). A characteristic plot of R against I is shown in Fig. 5.

To calculate the velocity D of the induced-transparency wave relative to the "cold" metal it is necessary to use the conservation laws for the energy, momentum, and matter fluxes through the transparency front, in analogy with the procedure used in Sec. 1 to

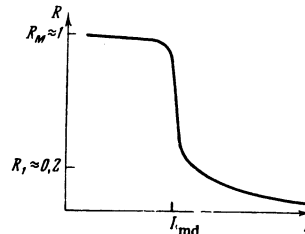


FIG. 5

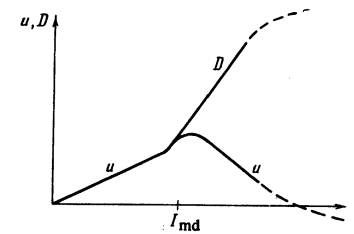


FIG. 6

FIG. 5. Reflection coefficient R vs the incident-light intensity I . The decrease of R in the region $I \gg I_{md}$ is given by $R \sim 1/I^2$.

FIG. 6. Velocity of evaporation boundary u and velocity of induced-transparency wave D vs the incident-light intensity.

determine the velocity u of the evaporation wave. A system of equations similar to (6) yields in this case

$$I_1/j_2 = w(T) - w_2(T_2) + 1/2 D^2 (V^2/V_2^2 - 1), \quad (17)$$

where I_1 is the intensity of the radiation incident on the induced-transparency front; the values marked by the subscript 2 pertain to the "cold" metal (i.e., ahead of the transparency front; see Fig. 4); $j_2 = D/V_2$ is the flux of matter through the front. The difference between the specific enthalpies in the right-hand side of (17) can be represented in the form

$$w(T) - w_2(T_2) = \lambda(T_2) - \lambda(T) + w_1(T) - w_1(T_2) = \lambda(T_2) - \lambda(T) + 5(T - T_2)/2M, \quad (18)$$

where the subscript 1 pertain to the vapor and $\lambda(T) \equiv w_1(T) - w(T)$ is the specific heat of evaporation of the transparent matter at the temperature T ; analogously, $\lambda(T_2) \equiv w_1(T_2) - w_2(T_2)$ is the heat of evaporation (sublimation) of the solid metal at the temperature T_2 . Since the heat of evaporation λ does not experience a jump when matter goes from the metallic state into the dielectric state, the difference is

$$\lambda(T_2) - \lambda(T) \approx -(d\lambda/dT)_{T=T_2}(T - T_2) = (C - C_p)(T - T_2) \approx (T - T_2)/2M. \quad (19)$$

Substituting (18) and (19) in (17) and recognizing that $T = T_{md} \approx T_c$ and that $T_c \gg T_2$, we obtain

$$D = V_2 \frac{I_1}{3T_c/M + 1/2 D^2 [(V/V_2)^2 - 1]}. \quad (20)$$

The density jump V/V_2 in this formula must be regarded as specified by the induced-transparency condition, i.e., the condition $\xi \ll 1$. It is seen from (20) that at the start of the induced-transparency regime, when the excess of the intensity I over the threshold I_{md} is not too large, namely

$$I_1 \ll (3T_c/M)^{1/2} V_2 \approx 2 \cdot 10^3 T_c^{1/2} / A^{1/2} \approx (0.3 - 1) 10^{10} \text{ W/cm}^2$$

(A is the atomic weight of the target material), the velocity D depends linearly on I . At large excesses above the induced-transparency threshold we have, in accordance with (20), $D \sim I^{1/3}$.

Let us estimate the intensity region in which the above-described picture of evaporation with an induced-transparency wave is valid. The threshold intensity I_{md} , according to (13), is apparently located for most metals in the interval $10^7 - 10^8 \text{ W/cm}^2$.¹³⁾ The upper intensity

¹³⁾ At such intensities, according to (3b), the regime of fully developed evaporation is realized at radiation pulse durations $\tau > 10^{-4} - 10^{-6}$ sec.

limit is imposed by the impossibility of having a transparency wave faster than the speed of sound C_0 in cold metal. From (20) at $D = C_0$ we obtain $I \approx \rho C_0^3 \sim 10^{11}/A^{1/2} \approx (1-3) \cdot 10^{10} \text{ W/cm}^2$. This upper intensity limit is, of course, not fundamental from the physical point of view. The foregoing arguments apply also to the region $I > 10^{10} \text{ W/cm}^2$, but would be meaningless, since there exist stronger limitations (see below) than those considered here, due to other physical processes that must be taken into account in the region $I = 10^9 - 10^{10} \text{ W/cm}^2$.

We note that the transparency wave that appears when the intensity I of the incident radiation increases monotonically acquires immediately a finite velocity D . The reason is that the induced-transparency wave can be produced in fact (can be "detached" from the evaporation wave) only if the evaporation-front velocity relative to the stationary reference frame (i.e., relative to the "cold" metal)

$$u = \frac{(1-R_1)I_{md}V - D\left(\frac{V}{V_2} - 1\right)}{\lambda_1/M} \quad (21)$$

is smaller than the velocity of the induced-transparency wave relative to the same reference frame, i.e., D .¹⁴⁾

On the basis of (20), this yields the condition $I_1 > (3T_c/\lambda_1)(1-R_1)I_{md}$; since $R \approx R_1$ at the start of the induced-transparency regime and accordingly $I_1 \approx (1-R_1)(I - I_{md})$, the "detachment" of the induced-transparency wave should set in at $I > (1 + 3T_c/\lambda_1)I_{md}$. We note that $3T_c/\lambda_1 \approx 0.3$.

Figure 6 shows a plot of the velocity u of the evaporation-wave front and of the velocity D in the laboratory frame against the intensity I of the radiation incident on the target. At $I < I_{md}$ the $u(I)$ plot is determined by formula (1). The strong deviation of $u(I)$ from linearity in the vicinity of the threshold point I_{md} (to its left) is due to the sharp increase of the absorptivity $(1-R)$ of the target surface from the value $1 - R_m$ to the value $1 - R_1$. At $I > I_{md}$, the function $u(I)$ is determined by formulas (20) and (21). At $I \approx I_{md}$, the velocity u has a maximum. Further increase of I leads first to a stopping of the evaporation front ($u = 0$), followed by its motion away from the "cold" metal ($u < 0$). The described behavior of the velocity u can also serve as a basis for an experimental investigation of the considered induced-transparency effect.

We have considered above the simplest metal evaporation mechanism at high intensities of the incident light $I > I_{md}$, when transparency is induced in the target material (Fig. 4). At the same time it is necessary to take into account certain physical processes which have not been taken into account in the described picture and can change the limits of applicability of the developed theory, and also modify the picture in question.

In experiments with millisecond laser pulses with light-flux intensities $I \gtrsim 10^9 \text{ W/cm}^2$, it is necessary to take into account for most metals the possible occurrence of appreciable ionization in the liquid-dielectric layer and the subsequent development of strong absorption in it during the time of the radiation pulse.

¹⁴⁾This additional condition was not taken into account in (17), and therefore there are no formal lower bounds on the intensity I_1 in formula (20).

A significant influence can be exerted also by a finite volume absorption of light in the dielectric albeit small in comparison with the metallic absorption. If the absorption coefficient μ_d is large enough, so that during the time τ of the radiation pulse the optical thickness is $\mu_d(D-u)\tau \gg 1$, then the induced-transparency wave can be observed only at the beginning of the pulse, during a time interval $t \ll \tau$.

Another important circumstance that limits the possibility of observing the induced-transparency wave may be the metastable character of the equilibrium of the liquid dielectric, in which the pressure, as noted above, is approximately half the saturated-vapor pressure at the given temperature¹⁵⁾. In order for a transparency wave to exist in the form corresponding to Fig. 4, the lifetime of the metastable state of the superheated dielectric liquid must not exceed the duration of the radiation pulse. This time is determined by the presence of nuclei of volume boiling (e.g., bubbles of critical dimension or ions resulting from thermal ionization), the number of which is larger the closer the temperature T_{md} is to the critical temperature T_c . For metals with high values of T_c and with small differences $(T_c - T_{md})$, intense volume boiling can develop in the dielectric liquid layer, and this should lead in the stationary situation to a reduction of the dimensions of this layer and thus considerably distort the picture shown in Fig. 4. Contributing to the violation of the metastable equilibrium is possible absorption in the dielectric layer, which brings its temperature closer to critical.

The questions noted here call for further analysis and for additional experimental material. Nonetheless, the available experimental facts (see Sec. 4) indicate quite convincingly, from our point of view, the existence of a transition of the liquid metal into a liquid dielectric state in experiments on the evaporation of metals by laser radiation.

3. EJECTION OF MATTER AND TARGET RECOIL MOMENTUM

The simplest experiments that yield information on processes occurring on a target are measurements of the reaction recoil momentum of the vapor¹⁶⁾ and of the mass of material ejected from the target during the time of the laser pulse. These quantities are determined only by the conditions on the boundary between the phases and are not connected with the subsequent motion of the vapor if the screening of the light incident on the target has a constant (or zero) value. The experimental data are usually presented in the form of plots of the recoil momentum J and of the ejected mass Δm , divided by the total energy E_0 in the radiation pulse, as functions of the laser-radiation intensity. The recoil momentum is $J = PS\tau$, and the mass is $\Delta m = j_1 S\tau$, where S is the area of the irradiated spot, $P = 0.56P_S$ (P_S is the pressure on the target boundary) (see (10)), and the density of the vapor stream is $j_1 = 0.82j_{vac}$, where j_{vac} is given by formula (4). The total energy E_0 generated

¹⁵⁾This circumstance was pointed out to us by A. A. Samokhin.

¹⁶⁾The occurrence of a reaction momentum due to the ejection of vapor from the target when acted upon by laser radiation was first pointed out in [19].

in one pulse is connected with the energy E incident on the target by the relation

$$E_0/E = I_0/I = e^\theta; \quad I_0 = E_0/S\tau,$$

where the optical thickness θ , as explained at the end of Sec. 1, depends little on I and is close to unity.

In the intensity region $I < I_{md}$ we obtain on the basis of (5) and (4) the following expressions for the relative values J/E_0 and $\Delta m/E_0$:

$$J/E_0 = 4.2 e^{-\theta} (M/\lambda_1) \sqrt{T/2\pi M} (1-R), \quad (22)$$

$$\Delta m/E_0 = e^{-\theta} (M/\lambda_1) (1-R) \quad (23)$$

(λ_1 is the heat of evaporation per particle). We see therefore that in the considered evaporation regime the relative values J/E_0 and $\Delta m/E_0$ are determined only by the specific heat of evaporation of target material at $T = T_0$, and are practically independent of the beam intensity I_0 .¹⁷⁾ It should be noted that the experimental values of J/E_0 make it possible, in accordance with (22), to determine the target surface temperature (if the optical thickness θ is known in this case).

We consider now the region of high intensities $I > I_{md}$. In the immediate vicinity of the point $I = I_{md}$ there should be observed a sharp increase of J/E_0 and $\Delta m/E_0$, by a factor $(1-R_1)/(1-R_M)$. At $I \approx I_{md}$ (and accordingly $T \approx T_{md}$), J and Δm reach the maximum values possible for the given material:

$$J_{max} = 0.56 P_s(T_{md})S\tau \approx (P_c/2)S\tau,$$

$$(\Delta m)_{max} = \frac{(1-R_1)I_{md}}{\lambda_1/M} S\tau \approx P_c \sqrt{\frac{M}{2\pi T_k}} S\tau.$$

With further increase of the intensity $I > I_{md}$, the values of J and Δm remain constant, and consequently the relative values J/E_0 and $\Delta m/E_0$ decrease like $1/I_0$. This is physically understandable, since at $I \gg I_{md}$ the bulk of the energy is consumed in heating a layer of metal to a temperature T_{md} and in moving the induced-transparency wave into the interior of the target.

Thus, the experimentally observed dependence of the relative recoil momentum J/E_0 on the radiation intensity $I_0 = E_0/S\tau$ should have a maximum at $I \approx (I_0/e^\theta) \approx I_{md}$, due to the onset of evaporation with induced transparency of the metal (transition from a liquid metal to a liquid dielectric). Such a singularity in the behavior of the dependence of J/E_0 on I_0 can serve as one more (third) basis for an experimental observation of the effect.

The results are confirmed experimentally by the data given in Sec. 4.

4. EXPERIMENTAL RESULTS

We present below experimental results pertaining to the aforementioned physical phenomena in the target.

Measurements on bismuth and lead targets have shown that the relative recoil momentum as a function of the incident intensity first goes through a maximum followed by a decrease with increasing I_0 , due (in accordance with the results of Secs. 2 and 3) to the onset of a liquid metal—liquid dielectric transition.

¹⁷⁾ A weak dependence of J/E_0 and of $\Delta m/E_0$ on I_0 in the case of fully developed evaporation was first noted in [20].

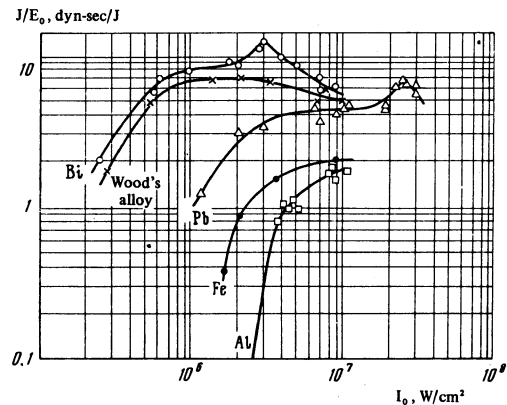


FIG. 7. Experimental plot of the relative recoil momentum J/E_0 against the incident-radiation intensity I_0 for aluminum, iron, lead, Wood's alloy, and bismuth.

A distinguishing feature of our experiments was the use of a laser of high emission energy. The lasers used in earlier studies of metal evaporation had energies not higher than 1 kJ at radiation pulse durations $\tau \sim 10^{-3}$ sec. It was therefore necessary to focus the beam sharply on the target in order to obtain a flux 10^6 – 10^7 W/cm². Consequently, the conditions realized in the experiment differed noticeably from the one-dimensional evaporation model considered in the theory. The depth h of the crater produced in the target by the radiation was much larger than the diameter d of the irradiated spot, and edge effect due to the washing out and directional ejection of liquid metal from the walls of the crater made large contributions to the measured quantities. In our experiments we used a neodymium-glass laser with emission energy up to 10 kJ in a pulse of duration $\tau = 0.8 \times 10^{-3}$ sec,¹⁸⁾ making it possible to work with large spots, $d \gg h$. The edge effects were then negligible.

The spot diameters were not less than 0.7 cm up to an intensity 3×10^7 W/cm²; the ratio d/h in the worst case (for aluminum) was ≈ 3 . Focusing was with a lens of focal length $f = 1$ – 1.5 m.

The recoil momentum was determined from the deflection of a ballistic pendulum on which the target was mounted, and the ejection of the target mass was determined by weighing the target before and after irradiation. The experiments were performed in air at atmospheric pressure. The intensity I_0 at the target was varied by changing the laser pump level and the dimension of the irradiated spot.

The experimental plots of the recoil momentum per unit incident energy J/E_0 and of the relative ejected mass $\Delta m/E_0$ against the incident power flux I_0 are shown for different metals in Figs. 7 and 8.

The curves agree with the theory developed in the preceding sections. The onset of evaporation has a threshold character. There are flux regions corresponding to the liquid—vapor phase transition far from the point at which the induced transparency regime begins. In these regions, the values of J/E_0 and $\Delta m/E_0$ are almost constant. The experimental values of J/E_0 at intensities lower than I_{md} agree well with those calculated from formula (22) at $\theta \approx 1$. For bismuth the calcu-

¹⁸⁾ A detailed description of the setup is given in [21].

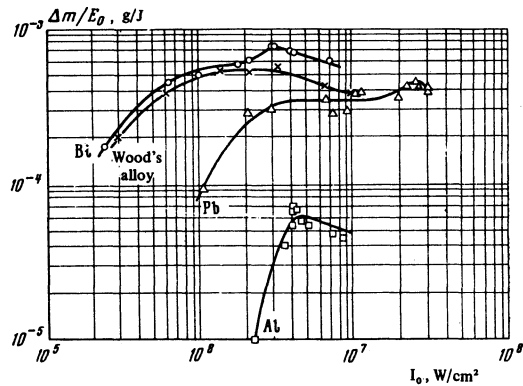


FIG. 8. Experimental dependence of the relative ejected mass $\Delta m/E_0$ on the intensity I_0 of the incident radiation for aluminum, lead, Wood's alloy, and bismuth.

lations yield $J/E_0 = 7-7.4$ dyn-sec/J in the interval $I_0 = (0.9-2.5) \times 10^6$ W/cm², and for aluminum $J/E_0 = 1.1-1.23$ dyn-sec/J in the region $I_0 = (0.8-2.4) \times 10^7$ W/cm². The agreement between the calculated and observed values of J/E_0 indicates that the estimate of the absorption of light in vapor, given at the end of Sec. 1, is correct, for without allowance for the factor $e^{-\theta}$ ($\theta \approx 1$) the theoretical values of J/E_0 would exceed the experimental ones by approximately 4 times.

Let us compare the curves for bismuth and lead in the region $I < I_{md}$. The thermophysical parameters of these metals, which enter in formula (22), are very close; the only difference is in the reflection coefficients. For liquid lead at 1.06μ we have according to^[22] a value of 73% for R_{Pb} as against about 50% for R_{Bi} of bismuth. Therefore the ratio of the reaction momentum in the region where $J/E_0 \approx \text{const}$ is $(J/E_0)_{Bi} : (J/E_0)_{Pb} = (1 - R_{Bi}) / (1 - R_{Pb}) \approx 2$, as is indeed observed in the experiments.

The $\Delta m/E_0$ curves deviate from the calculated values. The experimental data are approximately three times larger than the calculated ones at $\theta \approx 1$. The reason for this lies apparently in the fact that an appreciable fraction of the mass is carried away from the target in the form of drops of liquid metal, which are scattered predominantly tangentially to the surface of the target without contributing to the recoil momentum. At the same time, the curves shown in Fig. 8 confirm qualitatively the conclusions of the theoretical part of the paper.

New data were obtained for the first time at higher intensities. The curves for Bi and Pb (Fig. 7) show clear maxima indicating that a surface temperature $T \approx T_{md}$ is reached at the corresponding intensities. We note that the experimental values of J/E_0 at the maxima exceed the momenta at $I < I_{md}$ by 50-60%, which is close to the theoretical expected value $(1 - R_1) / (1 - R_M)$ if we put $R_1 \approx 0.2$. The values of $(I_0)_{md}$ are 3×10^6 W/cm² for bismuth and 2.5×10^7 W/cm² for lead.

Using the plot of Fig. 2, we can obtain the temperature T_{md} , which equals $\approx 2500^\circ\text{K}$ for bismuth and $\approx 3350^\circ\text{K}$ for lead.

Experiments directly confirming the existence of a sharp drop of the reflection coefficient R with increasing intensity I incident on the target (silver, copper, steel) are described in^[6]. The measurements have shown that when intensities on the order of 10^7-10^8

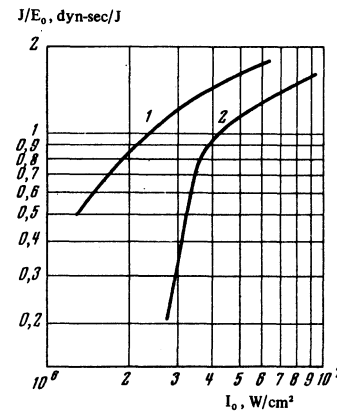


FIG. 9. Experimental plots of the relative recoil momentum J/E_0 for aluminum as a function of the incident radiation, obtained at a radiation energy $E_0 \lesssim 1$ kJ (curve 1) and at $E_0 \lesssim 10$ J (curve 2).

W/cm² are reached in an individual spike of a millisecond laser pulse, the reflection coefficients for all the employed targets decrease by an approximate factor of 5. The theoretical interpretation proposed in^[6] for these results, based on a simple allowance for the temperature dependence of the metallic conductivity, is patently inconsistent, since it calls for a final heating of the target surface to temperatures greatly exceeding the critical value. The results of the theoretical analysis in Sec. 2 of the present paper agree quite satisfactorily with these experimental data. Indeed, for such "good" metals as silver and copper, according to our estimates, it follows that $(R_1/R_M) \approx 1/5$. On the other hand, at $I \gtrsim I_{md}$ the decrease of the reflection coefficient, as shown above, slows down. In the experiments, therefore, one always should observe approximately such a decrease of R for such metals, as soon as $I \gtrsim I_{md}$. As to steel, one can speak only of a qualitative agreement with our ideas.

When I rises above I_{md} , a decrease of J/E_0 (and also of $\Delta m/E_0$) sets in both for bismuth and for lead, approximately like $1/I_0$ as predicted by the theory. (An exception is Wood's alloy, whose maximum is smooth and whose decrease is slower than $1/I_0$.)

Our results together with the already noted results of measurements of the reflection coefficient (6) are, in our opinion, an experimental confirmation of the liquid metal-liquid dielectric phase transition described in Sec. 2, which occurs when a metallic target is evaporated by a laser beam.

As follows from Fig. 2, the surface temperature of aluminum is close to T_c already at an intensity 3×10^7 W/cm². We did not observe, however, the theoretically predicted dependence of J/E_0 on I_0 in this region. There is, however, a known experimental study whose results can apparently be interpreted from the point of view of the metal-dielectric transition in aluminum. A study^[7] of the growth of the depth of the crater during the time of a pulse with $\tau \sim 10^{-3}$ sec has shown that starting with an intensity $I_0 = 2.5 \times 10^7$ W/cm² the maximum depth produced after the total irradiation time remains constant with increasing I_0 up to a value $I_0 = 4 \times 10^7$ W/cm². This can be attributed to the induced transparency of the metal and to the fact that the evaporation front reaches the maximum velocity $u(T_{md})$ (see Sec. 2).

The reason why our measured recoil momentum of

aluminum shows no singularities connected with induced transparency may be that aluminum is the only metal used in our experiments in which the depth of the crater is relatively large, and the reliable experimental points obtained under conditions of planar evaporation lie below $I_0 = 10^7$ W/cm². As already mentioned at the beginning of this section, failure to satisfy the condition $h \ll d$ gives rise to edge effects that lead, in particular, to an increase of the recoil momentum as the result of directed ejection of liquid metal. This is apparently the very reason why no singularities of J/E_0 and $\Delta m/E_0$ as functions of I_0 have been observed so far.

It should be noted that, even far from the induced transparency threshold values I_{md} and T_{md} , the values of J/E_0 and $\Delta m/E_0$ measured by us under conditions close to planar evaporation differ significantly from measurement obtained with sharp focusing. A comparison of the corresponding results in the case of aluminum is shown in Fig. 9. Curve 1 in this figure was obtained in our experiments with a laser whose emission energy was $E_0 \approx 1$ kJ. A certain difference between the results of experiments with sharp focusing and with larger spots is observed also in measurements of the mass of material ejected from the target surface. In^[23], where an emission energy up to 1 kJ was used, the results obtained for J/E_0 were higher, as in our experiments, than in the measurements shown in Fig. 7, where energies up to 10 kJ were used.

It is difficult to compare experimental data obtained under conditions of sharp focusing, since the shape of the crater can strongly influence the recoil momentum in this case. We performed the following experiment, which confirmed this influence. We measured the recoil momentum at a radiation energy up to 1 kJ, using lenses with focal lengths $f = 1$ m and $f = 0.3$ m. The target was located at the same distance from the focal plane of the lens in front of the focus in one case and behind it in the other. A converging light beam was incident on the target in the former case and a diverging one in the latter. At equal intensities and equal spots, the recoil momentum measured with the target located behind the focus was on the average larger than the momentum obtained when the target was in front of the focus. The shorter the focal length of the lens, the more noticeable this effect. In the case of the lens with $f = 0.3$ m, the data differed by an approximate factor of 2. The observed effect is due to the different shapes of the craters, the edges of the crater obtained behind the focus being sharply outlined, while those obtained in front of the focus are blurred. In the former case the ejection of matter (vapor or liquid) is therefore more directional and the recoil momentum is increased. The foregoing examples show how important it is to obtain conditions of planar evaporation in the experiments.

CONCLUSION

The results of^[24] reported here, pertaining to the vanishing of metallic properties of a target whose surface is heated by laser radiation of intensity $I > I_{md}$, and to the associated induced transparency of the material, which makes it impossible to heat the surface to a temperature above critical, are based at the present time on the following experimental data.

First, a sharp decrease of the reflection coefficient of the light at $I > I_{md}$ (see^[6] and Secs. 2 and 4 of the present article), and second, the anomalous dependence of the relative recoil momentum on the incident intensity, with a maximum at $I = I_{md}$ and with subsequent decrease at $I > I_{md}$, as found in the present work. A confirmation of the induced transparency of the metal may also be the fact that the velocity of the evaporation front as a function of I exhibits saturation in the experiments with aluminum (see^[7] and Sec. 2 of the present article). An additional confirmation of the conclusions of the present article can be found in experiments on the gas-dynamics of plasma flares. These experiments are not reported in the present article. We do present, however, a brief summary of their results pertaining to the main conclusions of the metal-evaporation theory described above.

It was shown earlier^[14] that when laser radiation of millisecond duration at sufficiently high intensity ($I_0 \sim 10^7$ W/cm²) acts on a target, the result is a gas dynamic plasma flare structure which is stationary in time, with a shock wave that is immobile relative to the target; the characteristic dimensions of the shock wave are much larger than the dimensions of the zone of target irradiation (if the pressure of the surrounding medium is $p \leq 1$ atm).

We have obtained the dependence of the flux j_1 of vapor from the target on the light intensity by measuring the velocity of the gas ahead and behind the shock-wave front, and also by measuring the distance between the shock wave and the target at different intensities of the incident light. Experiments with bismuth have shown that at $I_0 < (I_0)_{md} \approx 3 \times 10^6$ W/cm² (this value corresponds to the position of the maximum on the j/E_0 curve of Fig. 7) the value of j_1 agrees with that calculated from the formulas of Sec. 1 of this article, and at $I_0 > 3 \times 10^6$ W/cm² the $j_1(I)$ plot flattens out, as predicted by the theory of Sec. 2 of the article. We note that, unlike the method in which the ejected mass is determined by weighing the target before and after the experiment, this method eliminates the contribution of the liquid phase to the determined mass flow.

Other results having a direct bearing on the present study concern the absorption of the transmitted light by the plasma flare in the structure described above.

It was established in^[14] that under the experimental conditions $p \lesssim 1$ atm and $I_0 \sim 10^7$ W/cm² (Fig. 7) the absorption of light in the part of the flare behind the shock wave front is negligibly small. As to the absorption of the transmitted light near the target in the zone of one-dimensional planar scattering of the vapor, it follows from the stationary character of the gas dynamic structure and from the picture of the glow of the flare that if such absorption does take place it is approximately constant in magnitude ($\theta = \text{const}$). This means that the decrease of J/E_0 observed by us as a function of I_0 at $I > I_{md}$ for bismuth and lead (Fig. 7) is not connected with absorption of radiation in the flare. (The calculated and measured values of J/E_0 agree at $I < I_{md}$ when $\theta \approx 1$, see Secs. 3 and 4). This conclusion is important because, formerly, a plot of J/E_0 against I_0 similar to ours, with J/E_0 decreasing with increasing $I_0 > 10^9$ W/cm² in experiments in which the target is exposed to nanosecond laser pulses (see^[3], Sec. 5.3), is

connected precisely with the occurrence of strong screening of the target against the incident light by the development of optical breakdown of the vapor near the target.

The existence of a stationary regime of light absorption in our experiments in the region of one-dimensional motion of the vapor is by now an experimentally established fact. In experiments with bismuth targets under conditions corresponding to the data of Fig. 7, it was found that the velocity of the vapor in the region of one-dimensional scattering depends on the intensity like $u_1 \sim I_0^{1/2}$. The obtained absolute values of u_1 and the character of the $u_1(I_0)$ dependence, which is much stronger than in the phase-transition theory of Secs. 1 and 2, indicates that the vapor is heated in this region of motion to temperatures $T \sim 10^4$ K. Direct spectral measurements in the case of aluminum have shown, e.g., that at $I_0 \gg 10^7$ W/cm² the temperature of the vapor near the target is ≈ 1 eV, which is much higher than the critical temperature. This experimental fact, of course, does not contradict the results of the present article, which concern the impossibility of heating the target surface to a temperature above critical even if $I_0 \gg 10^7$ W/cm². The jump of the temperature in the region of one-dimensional vapor motion near the target takes place in a vapor "combustion" front which is stationary relative to the target.

Such an interpretation of the temperature jump is based on the experimentally demonstrated (see^[25]) possibility of maintaining a stationary plasma by a laser beam, a possibility based on processes analogous to slow chemical combustion.

¹J. F. Ready, J. Appl. Phys. **36**, 462, 1965.

²J. F. Ready, Proc. Nat. Electronics Conf., Chicago, October, 1964.

³S. I. Anisimov, Ya. A. Imas, G. S. Pomanov and Yu. V. Khodyko, *Deĭstvie izlucheniya bol'shoĭ moshchnosti na metally* (Effect of High-Power Radiation on Metals), Nauka, 1970.

⁴Yu. V. Afanas'ev and O. N. Krokhin, Trudy FIAN **52**, 118 (1970).

⁵L. D. Landau and E. M. Lifshitz, *Statisticheskaya fizika* (Statistical Physics), Nauka, 1964 [Addison-Wesley, 1969].

⁶A. M. Bonch-Bruevich, Ya. A. Imas, G. S. Romanov, M. N. Libenson and L. N. Mal'tsev, Zh. Tekh. Fiz. **38**,

851 (1968) [Sov. Phys.-Tech. Phys. **13**, 640 (1968)].

⁷I. G. Karasev, V. M. Kirillov, V. É. Norskiĭ, V. I. Samoilov, and P. I. Ulyakov, *ibid.* **40**, 1954 (1970) [15, 1523 (1971)].

⁸S. I. Anisimov, Zh. Eksp. Teor. Fiz. **54**, 339 (1968) [Sov. Phys.-JETP **27**, 182 (1968)].

⁹H. S. Carslaw and J. C. Jeager, *Conduction of Heat in Solids* (Russ. transl.) Nauka, 1964 [Oxford, 1959].

¹⁰R. C. Reid and T. K. Sherwood, *Properties of Gases and Liquids*, McGraw, 1966.

¹¹V. A. Alekseev, *Teplofizika vysokikh temperatur* **8**, 641 (1970).

¹²I. Z. Fisher, *Statisticheskaya teoriya zhidkosteĭ* (Statistical Theory of Liquids), Fizmatgiz, 1967.

¹³W. Llewellyn and V. Grabovskii, transl. in: *Atomnaya tekhnika za rubezhom*, No. 2, 14 (1962).

¹⁴V. A. Batanov, F. V. Bynkin, A. M. Prokhorov, and V. B. Fedorov, ZhETF Pis. Red. **11**, 113 (1970) [JETP Lett. **11**, 69 (1970)].

¹⁵I. K. Kikoin and A. P. Senchenkov, *Fizika metallov i metallovedenie* **24**, 843 (1967).

¹⁶Ya. B. Zel'dovich and L. D. Landau, Zh. Eksp. Teor. Fiz. **14**, 32 (1944).

¹⁷A. A. Brish, M. S. Tarasov, and V. A. Tsukerman, Zh. Eksp. Teor. Fiz. **38**, 22 (1960) [Sov. Phys.-JETP **11**, 15 (1960)].

¹⁸L. D. Landau and E. M. Lifshitz, *Élektrodinamika sploshnykh sred* (Electrodynamics of Continuous Media), Gostekhizdat, 1957 [Addison-Wesley, 1959].

¹⁹G. A. Askar'yan and E. M. Moroz, Zh. Eksp. Teor. Fiz. **43**, 2318 (1962) [Sov. Phys.-JETP **16**, 1637 (1963)].

²⁰Yu. V. Afanas'ev and O. N. Krokhin, *ibid.* **52**, 966 (1967) [25, 639 (1967)].

²¹V. A. Batanov, B. V. Ershov, L. P. Maksimov, V. V. Savranskii, and V. B. Fedorov, *Kratkie soobshcheniya po fizike*, no. 4 (1970).

²²Yu. V. Afanas'ev, N. G. Basov, O. N. Krokhin, N. V. Morachevskii, and G. V. Sklizkov, Zh. Tekh. Fiz. **39**, 894 (1969) [Sov. Phys.-Tech. Phys. **14**, 669 (1969)].

²⁴V. A. Batanov, F. V. Bunkin, A. M. Prokhorov and V. B. Fedorov, FIAN Preprint No. 22, 17 February 1972.

²⁵F. V. Bunkin, V. I. Konov, A. M. Prokhorov, and V. B. Fedorov, ZhETF Pis. Red. **9**, 609 (1969) [JETP Lett. **9**, 371 (1969)].

Translated by J. G. Adashko

62